The influence of low-energy particle–surface interactions on the initial stages of thin film formation

C. A. Stone and N. M. Ghoniem
Mechanical, Aerospace, and Nuclear Engineering Department, UCLA, Los Angeles, California 90024

(Received 20 September 1990; accepted 8 October 1990)

The initial stages of thin film formation by energetic particle deposition are modeled by a system of kinetic rate equations which describe atomic clustering phenomena. Specifically, a set of discrete kinetic rate equations, used to model small atomic clusters, is coupled to a set of kinetic moment equations which describe the size distribution function of large atomic clusters. These moments are derived from a Fokker–Planck equation which is an equivalent continuum limit of the discrete kinetic clustering equations. Low-energy particle–surface interactions and their impact on the growing film are considered by modeling surface defect production, sputtering, and cluster dissolution effects. Comparisons are made with thermal atom deposition to demonstrate the influence of energetic particle bombardment on the cluster size distribution, total cluster density, and nucleation rate.

I. INTRODUCTION

A number of energetic particle deposition processes are currently being used for surface modification and thin film production purposes. These processes use a high vacuum system to condense superthermal free particles onto a host substrate material, or alternatively, stimulate the deposition process by some means of energetic particle bombardment. As a result, energetic deposition techniques can influence film growth with a variety of synergistic effects that are absent during thermal deposition.[1] Such processes impact both the substrate and the growing film, and include such physical mechanisms as sputtering, implantation, reflection, defect production, collisional mixing, and heating. If a plasma is used during the deposition, the nature and chemistry of the deposited species can also be changed. Consequently, thin film formation with energetic particle bombardment is fundamentally different from atomistic deposition processes involving only thermal particles.

Low-energy (often <100 eV) deposition experiments have been used to control the growth kinetics and thus the physical properties of thin films, resulting in a number of interesting features. These features include film densification and increased oxidation resistance in optical films; minimization or elimination of columnar microstructure in metallization layers used in electronic devices; alteration of the state of stress, average grain size, and preferred grain orientation; increased film/substrate adhesion; enhanced conformal coverage; control of magnetic anisotropy in recording layers; epitaxial growth at lower temperatures; stimulation of surface chemical reactions; tailored film compositions; deposition of selective species; growth of metastable phases; and increased dopant incorporation probabilities (with a corresponding decrease in segregation-induced broadening of dopant profiles) in molecular-beam epitaxy (MBE)-grown Si and III–V semiconductors.[2,3] Nonetheless, one desired feature may be accompanied by several deleterious features, jeopardizing the utility of a specific thin film application. Thus, in an effort to better clarify the impact of the energetic species and to assess the role of experimental parameters, the study of energetic particle bombardment during thin film formation needs to be approached at a more fundamental level.

Three excellent review articles[3–5] provide a summary of experimental work performed over the past 15 to 20 years on the controlled use of low-energy particle bombardment on the early stages of film growth. These studies, however, often describe basic nucleation phenomena with conflicting results. For example, the nucleation rate and density of Ge clusters have been found to increase or decrease with ion irradiation, depending upon the choice of substrate material and substrate temperature used for the deposition.[6] Substrate "hardness" and thermal conductivity arguments were used to explain these discrepancies in terms of incident particle embedding effects and enhanced adatom mobility. The influence of particle bombardment on average cluster size is also subject to debate. Studies on thermal In and partially ionized In^+ beam experiments, used to deposit In islands on amorphous Si_3N_4 substrates at room temperature in an ultrahigh vacuum (UHV) MBE system, report a decrease in island number densities in the presence of ion irradiation which leads to larger average island sizes.[7] The authors attribute this irradiation effect to the loss of small clusters by sputtering and ion-induced dissociation. On the other hand, studies of Ar^+ ion bombardment during room temperature growth of Ag films reveal that irradiation decreases grain size, thus indicating that energetic particle deposition promotes smaller average cluster sizes.[8] Since an understanding of fundamental nucleation kinetics leads to the ultimate control of film growth, such discrepancies need to be resolved.

The nucleation and growth of gold clusters on sodium chloride substrates has been systematically studied because of the inert properties of gold, the ease with which well-defined surfaces can be obtained by cleaving NaCl single crystals, and the excellent resolution of Au clusters under electron microscopy. Thermal deposition studies of the Au/NaCl system have been used to investigate the initial stages of nucleation and growth,[9] the mobility and coalescence of Au nuclei,[10,11] as well as cluster size[12] and spatial[13] distributions. Inconsistencies in several such thermal depo-

 0734-2101/91/030759-09$01.00

sition studies led to the realization that the creation of preferred surface sites, induced by low-energy electrons originating in the Au vapor source, inadvertently influenced the nucleation kinetics.[14,15] Electron bombardment of a NaCl surface, during the evaporation of Au, has also been shown to lead to increased maximum island densities.[16]

Energetic Au/NaCl deposition studies have also been performed. High-energy ion beam sputtering systems have been used to sputter Au targets onto NaCl substrates. Observed increases in the maximum number density of Au islands, compared with results for thermal evaporation, can be quantitatively described by the generation of preferred nucleation sites on the substrate during the deposition.[17,18] The nucleation kinetics also depend on the angle at which the sputtered gold atoms strike the NaCl surface; Au atoms deposited at normal incidence have been shown to produce larger island densities than atoms bombarding the substrate at angles 60° to the normal.[19] Radio-frequency (rf) sputtering systems, which complicate matters by introducing plasma effects and the presence of a sputtering gas into the deposition environment, have also been used to study Au/NaCl nucleation phenomena. Harsdorff and Jark[20] rf-sputtered gold atoms onto NaCl substrates in a helium atmosphere, observing increased nucleation rates and island densities as compared to thermal evaporation works. Cluster size distributions were measured which appeared to be "quite similar to distributions from evaporation experiments" described by Schmeisser.[12] Magnets placed directly in front of the substrate surface were used to minimize crystal damage and heating that would occur as a result of electron and ion charged particle bombardment; however, the substrate remained open to backscattered neutral helium bombardment which could have influenced their results.

In this paper, a theory is presented which models the early stages of thin film formation by energetic particle deposition. Although a large number of synergistic effects influence the film growth process, energetic particle bombardment will be assumed to manifest itself in the following additional mechanisms: surface defect production, sputtering, and cluster dissolution. Comparisons with thermal evaporation studies will demonstrate the influence of energetic particle deposition on fundamental nucleation kinetics. Hopefully, some of the discrepancies in the current literature can be resolved.

II. MODEL DESCRIPTION

Developing a realistic theoretical model of a complex physical system requires an understanding of how the system evolves with respect to space and time, knowledge of the relevant components which constitute the system, and insight into the physical phenomena which govern system behavior. Mathematical equations can usually be formulated which describe the intricacies of the system; however, their solution may be intractable, depending upon the simulation details. The resourceful modeler is then faced with the arduous task of deciding which processes can be relaxed and which solution technique is most appropriate, without sacrificing the integrity of the work.

The study of thin film formation by energetic particle deposition represents a complicated physical system whose time evolution can be delineated by five distinct growth stages. During the first stage, the deposition species is transported through the deposition environment (e.g., vacuum, plasma, etc.) to the substrate surface, where it can participate in or be influenced by a number of physical processes. After a certain induction time, enough particles will have condensed on the substrate so that nucleation and growth can proceed. This marks the onset of the second stage, where both cluster density and size increase with time, virtually unaffected by neighboring clusters. A saturation stage arises when the cluster density has reached the maximum value that the substrate can accomodate for the given deposition conditions. Clusters continue to grow in size, but now coalesce with one another, producing a rapid decrease in cluster density. In the final stage, a continuous film forms; this is ultimately followed by multilayer growth.

In this model of thin film formation, the deposition source is assumed to produce a monoenergetic single-particle species of energy E, consisting of either charged particles or fast neutrals, which strike the substrate at a rate of q particles/unit area/unit time. Particle–surface interactions result in the creation of surface vacancies which will be denoted as *single traps* in this work. The quantity $C_T(t)$ denotes the number of single traps present on the substrate, per unit substrate area. These defects can trap a portion of the single-atom population that is initially accomodated on the substrate. The single-atom population $C(1,t)$ thus consists of a *bound* single-atom component $C_b(1,t)$ bound to defect sites, and a *mobile* single-atom component $C_{\text{mob}}(1,t)$ which can diffuse across the substrate. Nucleation and growth leads to the production of x-atom clusters, characterized by the cluster density $C(x,t)$.

Single traps, mobile and bound single atoms, and x-atom clusters are the basic constituents of our thin film system. The evolution of these species is governed by the following physical processes and general assumptions:

(1) Only monoenergetic, single particles of energy E are deposited.

(2) Point defects are generated at the rate $q\,p(E)$, where $p(E)$ is the average number of vacancy-interstitial pairs produced by each deposited particle. Only surface vacancies (i.e., traps) are created. $p(E)$ depends on the collision cascade generated by charged or neutral particle bombardment. Interstitial atoms are implanted well into the substrate (at least >5 atomic layers) and thus are not considered to influence surface atomic clustering.

(3) If $E \geqslant E_{\text{eject}}$, single atoms will be sputtered off the substrate. E_{eject} is the energy required to eject a single atom off the substrate. Ballistic migration effects are not considered.

(4) Cluster growth and decay proceed via single–particle transitions. Coalescence reactions are not considered, thus the model is only valid for the early growth stages where less than 15% of the substrate is covered.

(5) Single traps are mobile, governed by a diffusion energy E_d^T. They aggregate with other species on the substrate at a rate $\nu_{T,i}(t)C_i(t)$ [where $i = T$, m, b, or x for other traps, mobile single atoms, bound single atoms, and x-atom clusters, respectively]. The "T,b" and "T,x" reactions are assumed to only influence the single trap population.

(6) Mobile single atoms are governed by a diffusion energy E_d. They aggregate with other species on the substrate at a rate $\nu_{m,i}(t)C_i(t)$.

(7) Bound single atoms and larger x-atom clusters ($x \geqslant 2$) are immobile.

(8) Thermal oscillations can evaporate mobile single atoms off the substrate. This is characterized by an adsorption energy E_a and residence time $\tau_a = \nu_a^{-1}$.

(9) Thermal oscillations can release bound single atoms from traps, creating mobile single atoms in the process. The activation energy E_T determines the bound single atom confinement time $\tau_T = \nu_T^{-1}$.

(10) Direct impingement of the deposit on single trap sites creates bound single atoms at the rate $\nu_{\text{imp},T}C_T(t)$.

(11) Direct impingement of the deposit on x-atom clusters produces $(x+1)$-atom entities at the rate $\nu_{\text{imp}}(x)C(x,t)$.

(12) Energetic particle bombardment dissociates x-atom clusters into $(x-1)$-atom clusters and mobile single atoms at the rate $\nu_{\text{diss}}(x,E)C(x,t)$.

III. MODEL EQUATIONS

The model description outlined in Sec. II can be used to derive a system of discrete kinetic rate equations which describe the early stages of thin film formation by energetic particle bombardment.[21] If the largest cluster contains $X_{\max}$ atoms, then a set of $(X_{\max}+2)$ coupled, nonlinear, stiff, ordinary differential equations must be solved. Since cluster sizes increase with time, $X_{\max}$ must also increase, which dictates that more equations be solved as the deposition proceeds. If one has limited computing resources (e.g., time or money), this poses quite a problem, since atomic clusters can easily contain many thousands of atoms.

To circumvent this problem, a Fokker–Planck-type continuum equation is derived for $X_c \leqslant x \leqslant X_{\max}$, where x denotes the number of atoms in an x-atom cluster.[21,22] A transition cluster size X_c is defined as the smallest size described by the continuum. Clusters containing X_c or more atoms are described by a continuum distribution function $C_{\text{con}}(x,t)$ which depends on the following characteristics of the distribution: $C_{\text{tot}}(t)$, the total density of clusters in the continuum; $\langle x \rangle(t)$ the average size of the continuum clusters; and $M_n(t)$, the nth central moment of the continuum distribution, where $2 \leqslant n \leqslant N$ and N is the number of moments used to reconstruct the distribution function. Thus, atomic clustering phenomena will be modeled by a set of discrete kinetic rate equations for $1 \leqslant x \leqslant (X_c - 1)$, coupled to a set of kinetic moment equations which characterize a continuum distribution for $X_c \leqslant x \leqslant X_{\max}$. In the discussion that follows, it will be seen that the early stages of film growth are described by a hybrid system of $(X_c + N + 2)$ kinetic rate equations for the following variables of interest: single traps $C_T(t)$; mobile single atoms $C_{\text{mob}}(1,t)$; bound single atoms $C_b(1,t)$; discrete x-atom clusters $C(x,t)$ for $2 \leqslant x \leqslant (X_c - 2)$; the total density of continuum clusters $C_{\text{tot}}(t)$; the average size of continuum clusters $\langle x \rangle(t)$; the central moments of the continuum $M_n(t)$ for $2 \leqslant n \leqslant N$; and the net number of particles deposited $X_{\text{depos}}(t)$. The size of this hybrid system of equations, $(X_c + N + 2)$, can be typically several thousand times less than the size of the original discrete clustering system containing $(X_{\max} + 2)$ equations, thus providing faster computations without a loss of accuracy.

Production and loss mechanisms governing the single trap population reveal that

$$\frac{\partial C_T(t)}{\partial t} = [qp(E) + \nu_{\text{imp}}(1)C_b(1,t)\Theta(E - E_{\text{eject}}) + \nu_T C_b(1,t)] - \nu_{\text{imp},T}C_T(t) - \Big[2\nu_{T,T}(t)C_T(t) + \nu_{T,m}(t)C_{\text{mob}}(1,t) + \nu_{T,b}(t)C_b(1,t) + \sum_{x=2}^{X_c-1} \nu_{T,x}(t)C(x,t) + \langle \nu_{T,x}(t) \rangle C_{\text{tot}}(t)\Big], \tag{1}$$

where $\Theta(z) = 1$ for $z \geqslant 0$ and $\Theta(z) = 0$ for $z < 0$. Traps are produced by the collision cascade, when bound single atoms are sputtered out of traps, and when thermal oscillations release a bound single atom from a trap site. Direct impingement creates bound single atoms, removing traps in the process. As traps migrate over the substrate, they are also destroyed as they encounter other traps, mobile and bound single atoms, discrete x-atom clusters, and clusters in the continuum distribution. The $\langle\ \rangle$ symbols are used to denote quantities which have been appropriately averaged over the continuum and evaluated at $x = \langle x \rangle(t)$. It should be noted that $\nu_{T,T}(t)C_T(t)$ is the rate at which two traps *aggregate* together, however, since two traps are lost during each interaction, the total *loss rate* is $2\nu_{T,T}(t)C_T(t)$. This di-trap production rate is assumed to be negligible so that the di-trap population is insignificant compared to the single trap density.

The mobile single atom population is characterized by

$$\frac{\partial C_{\text{mob}}(1,t)}{\partial t} = \Big[q + \nu_T C_b(1,t) + \sum_{x=2}^{X_c-1} \nu_{\text{diss}}(x,E)C(x,t)(1+\delta_{x2}) + \langle \nu_{\text{diss}}(x,E) \rangle C_{\text{tot}}(t)\Big] - \nu_a C_{\text{mob}}(1,t) - \Big(\nu_{\text{imp},T}C_T(t) + \nu_{\text{imp}}(1)\{C_{\text{mob}}(1,t) + C(1,t)[1 - \Theta(E - E_{\text{eject}})]\} + \sum_{x=2}^{X_c-1} \nu_{\text{imp}}(x)C(x,t) + \langle \nu_{\text{imp}}(x) \rangle C_{\text{tot}}(t)\Big) - \Big[\nu_{m,T}(t)C_T(t) + 2\nu_{m,m}(t)C_{\text{mob}}(1,t) + \nu_{m,b}(t)C_b(1,t) + \sum_{x=2}^{X_c-1} \nu_{m,x}(t)C(x,t) + \langle \nu_{m,x}(t) \rangle C_{\text{tot}}(t)\Big], \tag{2}$$

where $\delta_{ab} = 1$ if $a = b$ and zero otherwise. Mobile single atoms are produced by the deposition source, the release of bound single atoms from trap sites due to thermal oscillations, and from the dissociation of both discrete x-atom and continuum clusters. The δ function accounts for the fact that two mobile singles are produced when a two-atom cluster dissociates. Desorption, direct impingement, and aggregation processes deplete the mobile single-atom inventory. The total single-atom density is $C(1,t) = C_{\text{mob}}(1,t) + C_b(1,t)$. Similar to trap–trap aggregation in Eq. (1), the rate at which two mobile single atoms aggregate together is $\nu_{m,m}(t)C_{\text{mob}}(1,t)$, however, two mobile singles are lost in the process so the total loss rate is $2\nu_{m,m}(t)C_{\text{mob}}(1,t)$.

The kinetic equation for bound single atoms is somewhat simpler:

$$\frac{\partial C_b(1,t)}{\partial t} = [\nu_{\text{imp},T} + \nu_{m,T}(t)]C_T(t) - [\nu_T + \nu_{m,b}(t) + \nu_{\text{imp}}(1)]C_b(1,t). \quad (3)$$

Bound singles are created when the deposit directly impinges on a trap or as mobile single atoms diffuse to traps. Bound singles are destroyed when thermal oscillations release a bound single from a trap site. Aggregation of mobile singles with bound singles and direct impingement of the deposit on bound singles create two-atom clusters, destroying bound single atoms in the process.

A separate kinetic equation must be written for two-atom clusters:

$$\frac{\partial C(2,t)}{\partial t} = \frac{1}{2}[2\nu_{m,m}(t)C_{\text{mob}}(1,t)] + \nu_{m,b}(t)C_b(1,t) + \nu_{\text{imp}}(1)C(1,t)[1 - \Theta(E - E_{\text{eject}})] - [\nu_{m,2}(t) + \nu_{\text{diss}}(2,E) + \nu_{\text{imp}}(2)]C(2,t) + \nu_{\text{diss}}(3,E)C(3,t). \quad (4)$$

Two-atom clusters are produced when two mobile singles aggregate together, mobile and bound singles aggregate, and when a low-energy deposit ($E < E_{\text{eject}}$) directly impinges on the single-atom population. The factor of 1/2 is needed in the first term in order to avoid counting twice each encounter between two atoms from the same $C_{\text{mob}}(1,t)$ population. Aggregation, dissociation, and direct impingement reactions involving two-atom clusters, though, deplete the two-atom population. The dissociation of three-atom clusters produces two-atom clusters and mobile single atoms.

Larger discrete clusters are modeled with a general kinetic rate equation. For $3 \leqslant x \leqslant (X_c - 2)$,

$$\frac{\partial C(x,t)}{\partial t} = [\nu_{m,x-1}(t) + \nu_{\text{imp}}(x-1)]C(x-1,t) - [\nu_{m,x}(t) + \nu_{\text{diss}}(x,E) + \nu_{\text{imp}}(x)]C(x,t) + \nu_{\text{diss}}(x+1,E)C(x+1,t), \quad (5)$$

where cluster growth and decay proceed via single–particle transitions.

By taking the zeroth, first, and higher-order moments of our Fokker–Planck continuity equation,[21] the following kinetic rate equations can be derived to model continuum clusters for $x \geqslant X_c$:

$$\frac{\partial C_{\text{tot}}(t)}{\partial t} = \mathscr{J}(X_c,t) \quad (6)$$

$$\frac{\partial \langle x \rangle(t)}{\partial t} = \xi_1(t) + \langle \mathscr{F}(x,t) \rangle \quad (7)$$

$$\frac{\partial M_n(t)}{\partial t} = \xi_n(t) + \phi_n(t) + \psi_n(t), \quad 2 \leqslant n \leqslant N. \quad (8)$$

The final kinetic rate equation used in the model describes the net number of particles deposited on the substrate, $X_{\text{depos}}(t)$, where

$$X_{\text{depos}}(t) = \sum_{x=1}^{X_c - 1} xC(x,t) + \langle x \rangle(t)C_{\text{tot}}(t). \quad (9)$$

Taking the time derivative of Eq. (9) and extending Eq. (5) to $x = (X_c - 1)$, one can use a linear combination of Eqs. (2)–(7) to obtain

$$\frac{\partial X_{\text{depos}}(t)}{\partial t} = q - \nu_a C_{\text{mob}}(1,t) - \nu_{\text{imp}}(1)C(1,t)\Theta(E - E_{\text{eject}}) + \tfrac{1}{2}\mathscr{F}(X_c,t)C(X_c,t). \quad (10)$$

From a physical standpoint, the net number of particles deposited on the substrate should be a balance between the deposition rate and losses due to evaporation and sputtering. An additional term arises, however, because of the hybrid coupling at $x = X_c$. Solving a kinetic equation for $X_{\text{depos}}(t)$ allows one to determine the unknown discrete cluster density $C(X_c - 1,t)$ as

$$C(X_c - 1,t) = \left(\frac{1}{X_c - 1}\right)\left[X_{\text{depos}}(t) - \sum_{x=1}^{X_c - 2} xC(x,t) - \langle x \rangle(t)C_{\text{tot}}(t)\right] \quad (11)$$

ensuring particle conservation in the model.

Additional functions and definitions are needed to close the preceding system of equations.[21] The nucleation current going into the continuum $\mathscr{J}(X_c,t)$ is

$$\mathscr{J}(X_c,t) = [\nu_{m,X_c-1}(t) + \nu_{\text{imp}}(X_c - 1)]C(X_c - 1,t) - \nu_{\text{diss}}(X_c,E)C(X_c,t) \quad (12)$$

while the drift and dispersion frequency functions at $x = X_c$, $\mathscr{F}(X_c,t)$ and $\mathscr{D}(X_c,t)$, are

$$\mathscr{F}(X_c,t) = \nu_{m,X_c}(t) - \nu_{\text{diss}}(X_c,E) + \nu_{\text{imp}}(X_c) \quad (13)$$

$$\mathscr{D}(X_c,t) = \tfrac{1}{2}[\nu_{m,X_c}(t) + \nu_{\text{diss}}(X_c,E) + \nu_{\text{imp}}(X_c)]. \quad (14)$$

The special nucleation frequency function $\xi_1(t)$ is

$$\xi_1(t) = \frac{[X_c - \langle x \rangle(t)]\mathscr{J}(X_c,t) + \mathscr{D}(X_c,t)C(X_c,t)}{C_{\text{tot}}(t)} \quad (15)$$

while the general nucleation $[\xi_n(t)]$, drift $[\phi_n(t)]$, and dispersion $[\psi_n(t)]$ frequency functions for $2 \leqslant n \leqslant N$ are

$$\xi_n(t) = \frac{\{[X_c - \langle x\rangle(t)]^n - M_n(t) - nM_{n-1}(t)[X_c - \langle x\rangle(t)]\}\mathscr{J}(X_c,t)}{C_{\text{tot}}(t)} + \frac{n\mathscr{D}(X_c,t)C(X_c,t)\{[X_c - \langle x\rangle(t)]^{n-1} - M_{n-1}(t)\}}{C_{\text{tot}}(t)} \tag{16}$$

$$\phi_n(t) = n\{\langle \mathscr{F}(x,t)[x - \langle x\rangle(t)]^{n-1}\rangle - M_{n-1}(t)\langle \mathscr{F}(x,t)\rangle\} \tag{17}$$

$$\psi_n(t) = n(n-1)\langle \mathscr{D}(x,t)[x - \langle x\rangle(t)]^{n-2}\rangle. \tag{18}$$

Quantities appearing within $\langle\ \rangle$ symbols have been averaged over the unknown continuum cluster distribution function and are determined from the N moments as

$$\langle g(x,t)\rangle = \left[g(x,t) + \sum_{n=2}^{N} \frac{M_n(t)}{n!}\frac{\partial^n g(x,t)}{\partial x^n}\right]_{@\,x=\langle x\rangle(t)}. \tag{19}$$

Physical processes are modeled with a number of characteristic clustering frequencies. The frequencies at which mobile single atoms $[\nu_{m,i}(t)]$ and single traps $[\nu_{T,i}(t)]$ aggregate with other species on the substrate [where $i = T, m, b,$ or x as described in Sec. II] are

$$\nu_{m,i}(t) = \frac{1}{4}a_0 a(1)\nu_1 \exp\left(-\frac{E_d}{kT}\right) \times C_{\text{mob}}(1,t)(1+\beta_{m,i})(1+\gamma_{m,i}) \tag{20}$$

$$\nu_{T,i}(t) = \frac{1}{4}a_0 a_T \nu_1 \exp\left(-\frac{E_d^T}{kT}\right) \times C_T(t)(1+\beta_{T,i})(1+\gamma_{T,i}) \tag{21}$$

where the diameters a_0, $a(1)$, and a_T characterize the size of the substrate atoms, deposit species, and single traps; ν_1 is an average vibrational frequency for both mobile single atom and single trap diffusive "hops" in *all* directions on the substrate; kT is the substrate temperature; and the β's and γ's are size and motion factors for a particular interaction.[21] The frequencies at which the deposit directly impinges on x-atom clusters and single traps are

$$\nu_{\text{imp}}(x) = q\frac{\pi a^2(x)}{4} \tag{22}$$

$$\nu_{\text{imp},T} = q\frac{\pi a_T^2}{4}. \tag{23}$$

The diameter of an x-atom cluster, $a(x)$, is

$$a(x) = a(1)x^r, \tag{24}$$

where r is the growth exponent, defined over $0 \leqslant r < 1$. A specific value for r dictates cluster geometry; for example, $r = 1/2$ describes two dimensional (2D) discs, while $r = 1/3$ describes three dimensional (3D) spheres.

Thermal oscillations can cause mobile single atoms to desorb off the substrate, as well as release bound single atoms from traps. The associated frequencies for these effects are

$$\nu_a = \nu_0 \exp\left(-\frac{E_a}{kT}\right) \tag{25}$$

$$\nu_T = \nu_2 \exp\left(-\frac{E_T}{kT}\right) \tag{26}$$

where ν_0 and ν_2 are characteristic vibrational frequencies.

The frequency at which x-atom clusters dissociate into $(x-1)$-atom clusters and mobile single atoms depends on the cluster size $a(x)$ as follows:

$$\nu_{\text{diss}}(x,E) = q\frac{\pi}{4}[a(x) + 2\lambda(E)]^2 \quad \text{for } a(x) < 2\lambda(E) \tag{27}$$

$$\nu_{\text{diss}}(x,E) = 2\pi q\lambda(E)a(x) \quad \text{for } a(x) \geqslant 2\lambda(E). \tag{28}$$

We define the parameter $\lambda(E)$ as the *mean free path for single-atom re-solution*. Cluster dissociation occurs when an energetic particle impinges within a distance $\lambda(E)$ from the edge of a cluster. It should be noted that the dissociation of small clusters does not require a direct impact if the cluster is within the collision cascade regime.[23] The outside edges of larger clusters can also be "chipped" off. Thus, a length of $\lambda(E)$ extends both inside and outside a cluster.

Up to this point, the continuum cluster distribution function remains unknown. Now it is a well-known property of a statistical distribution that if its moments are known, then the distribution itself is often completely determined. Orthogonal polynomials can be used to expand such distributions in terms of their moments. Using a series of Chebyshev–Hermite polynomials, the continuum cluster distribution function for $x \geqslant X_c$ is

$$C_{\text{con}}(x,t) = C_{\text{Norm}}(x,t)\left\{1 + \sum_{j=2}^{N} \mathscr{A}_j(t)\mathscr{H}_j[\rho(x,t)]\right\}, \tag{29}$$

based on using a total of N moments for the reconstruction. The normal distribution $C_{\text{Norm}}(x,t)$ is

$$C_{\text{Norm}}(x,t) = \frac{C_{\text{tot}}(t)}{\sqrt{2\pi M_2(t)}}\exp\left[-\frac{\rho^2(x,t)}{2}\right], \tag{30}$$

where

$$\rho(x,t) = \frac{x - \langle x\rangle(t)}{\sqrt{M_2(t)}}. \tag{31}$$

The Chebyshev–Hermite polynomials, $\mathscr{H}_j(z)$, are

$$\mathscr{H}_0(z) = 1,$$
$$\mathscr{H}_1(z) = z, \tag{32}$$
$$\mathscr{H}_j(z) = z\mathscr{H}_{j-1}(z) - (j-1)\mathscr{H}_{j-2}(z), \quad j \geqslant 2.$$

The expansion coefficients $\mathscr{A}_j(t)$ are

$$\mathscr{A}_j(t) = \theta(j,t) + \sum_{n=1}^{n_{\max}} \frac{(-1)^n\theta(j-2n,t)}{2^n n!} \tag{33}$$

where $n_{\max} = j/2$ for j even, $j \geqslant 2$, or $n_{\max} = (j-1)/2$ for j odd, $j \geqslant 3$. The moment ratio functions $\theta(j,t)$ are given by

$$\theta(j,t) = \frac{M_j(t)}{j!\left[\sqrt{M_2(t)}\right]^j}. \tag{34}$$

This hybrid system of kinetic clustering equations is completely closed by specifying

$$C(X_c,t) = C_{\text{con}}(X_c,t). \tag{35}$$

It should be recognized that previous kinetic rate equation formulations have been developed in order to interpret the results of deposition measurements which were influenced by the presence of surface defects. Lane and Anderson[18] used ion-beam sputtering to deposit Au on NaCl, measuring island densities as a function of substrate temperature and deposition rate. They were successful in interpreting their results in terms of a kinetic model which assumed a constant density of preferred adsorption sites. Usher and Robins[15] used a rate equation approach to analyze experiments in which preferred sites were continuously generated at a rate proportional to a power of the deposition rate. Using this approach, they were able to resolve several discrepancies in previous Au/NaCl nucleation measurements. Both of these studies developed analytical solutions to the film growth problem by making rather gross, time-independent estimates for cluster mobility effects. Direct impingement phenomena and particle–surface interactions were ignored, and neither solution provided any information on the cluster size distribution. Although many variables were experimentally difficult parameters to determine, the assumptions made in developing these analytical models are generally supported by their overall agreement with deposition measurements.

The kinetic rate equations outlined in this section can be numerically solved on a computer to obtain information about the nucleation kinetics and cluster size distribution characterizing the early stages of thin film formation by energetic particle bombardment. Surface defect production, sputtering, and cluster dissociation phenomena are modeled for an energetic deposition process, thus supplementing the aggregation and direct impingement events present in thermal deposition. The usefulness of this approach to nucleation and growth studies awaits experimental verification.

IV. RESULTS AND DISCUSSION

Low-energy particle–surface interactions can affect nucleation kinetics through the creation of preferred adsorption sites (e.g., traps), cluster dissociation, and surface sputtering. In this section, we present results for the individual roles that surface defect production and cluster dissociation have on the early stages of thin film formation. In the analysis of our computational results, it will be important to understand the nature, rather than the detail, of the nucleation phenomena.

For each simulation, deposition begins on a bare, defect-free substrate at time zero. Focusing on the early stages of the deposition process enables one to neglect direct impingement reactions on traps and clusters. Sputtering is also neglected. The vibrational frequencies ν_0, ν_1, and ν_2 are fundamental material constants of the order 10^{12} s^{-1}. Basing material-dependent parameters on the Au/NaCl system, we use $a(1) = 2.9\times10^{-8}$ cm as the diameter of the Au deposit

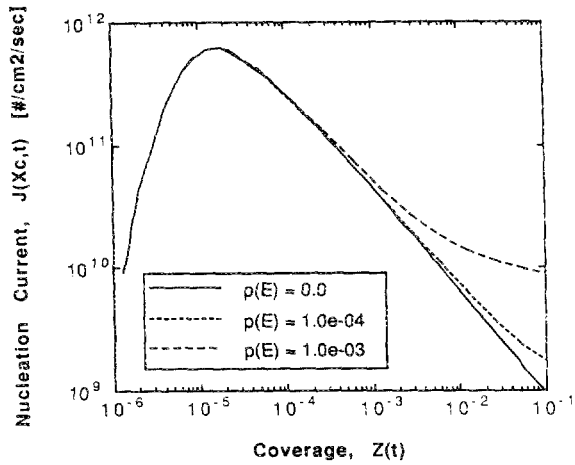

FIG. 1. The influence of surface defect production on the cluster nucleation rate $J(X_c,t)$ for the Au/NaCl system at 300 K. $p(E)$ is the average number of surface defects produced by each deposited particle.

and $a_0 = 2.8\times10^{-8}$ cm for the NaCl substrate. Surface defects are features of the substrate, thus we set $a_T = a_0$. In reality, the substrate atoms can relax around a trap, decreasing a_T, but this effect is ignored. Activation energies for the Au/NaCl system are taken to be $E_d = 0.16$ eV and $E_a = 0.48$ eV, based upon a consistent set of nucleation measurements for substrate temperatures between 123 and 448 K (Ref. 11). E_d^T is equivalent to an activation energy for surface-vacancy diffusion, taken to be 0.50 eV for this study. E_T is estimated to be $2E_a = 0.96$ eV, indicative of the increased binding provided by defect sites. The deposition rate is chosen to be $q = 10^{13}$ atoms/cm^2/s, and since Au nucleates as 3D entities on NaCl, $r = 1/3$.[24] For the continuum cluster size distribution, $X_c = 5$ and $N = 4$. A four-moment reconstruction allows one to model dispersion, skewness, and kurtosis in the distribution, features readily compared with experimental measurements.

The effect of surface defect production on the nucleation kinetics is first studied at 300 K under the assumption of no cluster dissociation, i.e., $\lambda(E) = 0$. Trap production is modeled with three values of $p(E)$ indicative of thermal $[p(E) = 0]$, low-energy $[p(E) = 10^{-4}]$, and high-energy $[p(E) = 10^{-3}]$ particle depositions. For clarity of presentation, we define the fractional substrate coverage $Z(t)$ as $X_{\text{depos}}(t)\pi a^2(1)/4$. Figure 1 demonstrates that surface defect production enhances the nucleation rate for coverages above 10^{-3}. This promotes an increase in the total cluster density, as shown in Fig. 2. It should be recognized that a certain incubation time is required, however, before changes in the nucleation phenomena are evident. This is clearly supported by Fig. 3, where cluster size distributions at deposition times of $t = 0.01$ s $[Z(t) \simeq 3\times10^{-5}]$ and $t = 20.0$ s $[Z(t) \simeq 0.13]$ are displayed. In Fig. 3(a), one cannot distinguish any differences in the calculated size distributions. As the deposition proceeds and traps have a chance to influence the kinetics, Fig. 3(b) illustrates that defect production reduces both the average cluster size and the range of cluster sizes present on the substrate.

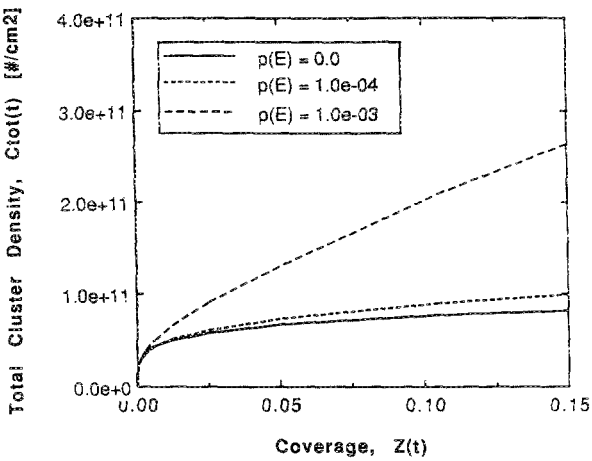

FIG. 2. The influence of surface defect production on the total cluster density $C_{tot}(t)$ for the Au/NaCl system at 300 K. $p(E)$ is the average number of surface defects produced by each deposited particle.

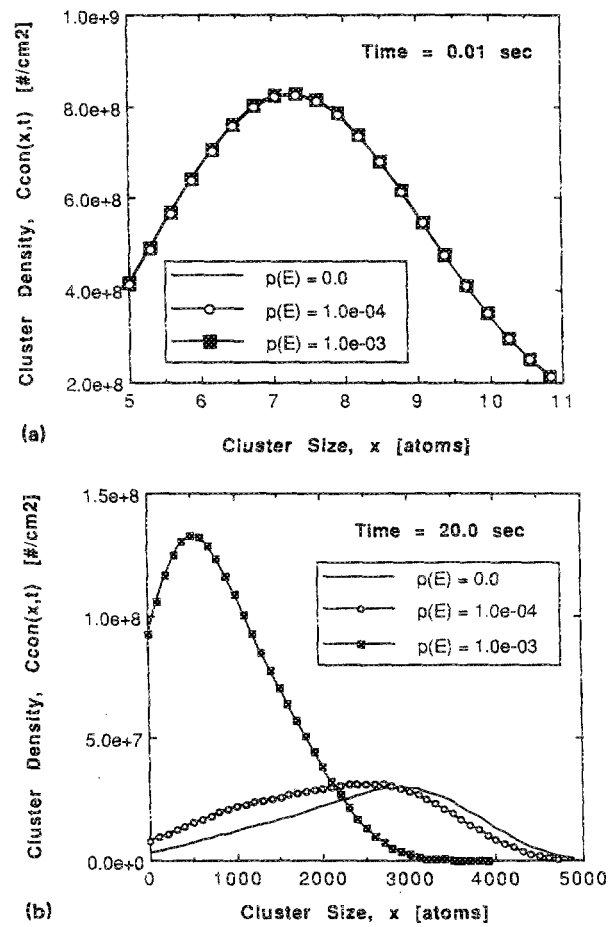

FIG. 3. (a) The influence of surface defect production on the calculated cluster size distribution at an early deposition time of $t = 0.01$ s, for the Au/NaCl system at 300 K. $p(E)$ is the average number of surface defects produced by each deposited particle. (b) The influence of surface defect production on the calculated cluster size distribution at a later deposition time of $t = 20.0$ s, for the Au/NaCl system at 300 K. $p(E)$ is the average number of surface defects produced by each deposited particle.

In summary, surface defect production creates preferred nucleation sites on a substrate, increasing the cluster nucleation rate, leading to larger nuclei densities and smaller cluster sizes. Films produced in this manner possess narrower size distributions, indicating that energetic particle bombardment can produce a more uniform distribution of cluster sizes during the early growth stages. It would be interesting to compare these trapping simulations to the case of accelerated ion doping during MBE experiments, where the ion flux is low, trapping is the desired effect, and sputtering of the growing film is not significant.[3]

Cluster dissociation effects on thin film growth kinetics are studied under the assumption of no surface defect production, i.e., $p(E) = 0$. Dissociation is modeled with two values of $\lambda(E)$ to simulate both thermal $[\lambda(E) = 0]$ and energetic $[\lambda(E) = 1.5 \times 10^{-8}$ cm] particle bombardment. It should be recognized that in this study, the dissociation mechanism competes with thermally activated processes, namely single-atom desorption and aggregation. Any observed effect that cluster dissociation has on the nucleation kinetics will thus be dependent upon the particular temperature used in the study. For the Au/NaCl system, experiments reveal that cluster mobility is a dominant process even down to a temperature of 133 K; dimers and larger clusters can only be considered immobile at temperatures below 128 K.[11] Since our current model considers that only single atoms are mobile (see assumptions 6 and 7 in Sec. II), we restrict our dissociation studies to substrate temperatures of 75, 100, and 125 K in order to be consistent with experimental observations.

During the early growth stages (e.g., less than 15% coverage) at the low substrate temperature of 75 K, dissociation promotes a decrease in the nucleation rate, leading to somewhat smaller cluster densities, as shown in Figs. 4(a) and 4(b). The destructive nature of the dissociation process also produces a *smaller* average cluster size, as well as a more disperse size distribution, as shown in Figs. 4(c) and 4(d). [The second moment $M_2(t)$ is equivalent to the variance of the size distribution.] At the higher substrate temperatures of 100 and 125 K, the thermally activated desorption and aggregation reactions become more prevalent. Our calculations indicate that cluster dissociation does not influence the nucleation kinetics at these higher temperatures.

Previous experiments studying the effect of ion bombardment on thin film growth have reported a decrease in the nucleation rate, leading to larger average cluster sizes.[7,25] These larger island sizes were attributed to a combination of ion bombardment effects which included enhanced adatom surface diffusion, sputtering, and the dissociation of small islands and clusters. Our low-temperature dissociation results, which do not consider enhanced adatom surface diffusion or sputtering, reveal that cluster dissociation decreases the nucleation rate (in agreement with the quoted experiments), but *decreases* the average cluster size. This discrepancy may be due to the fact that our model assumes that any x-atom cluster can dissociate, thus attributing too much importance to dissociation. Other ion bombardment experiments,[8] however, agree with our model calculations. Such differences require further investigation.

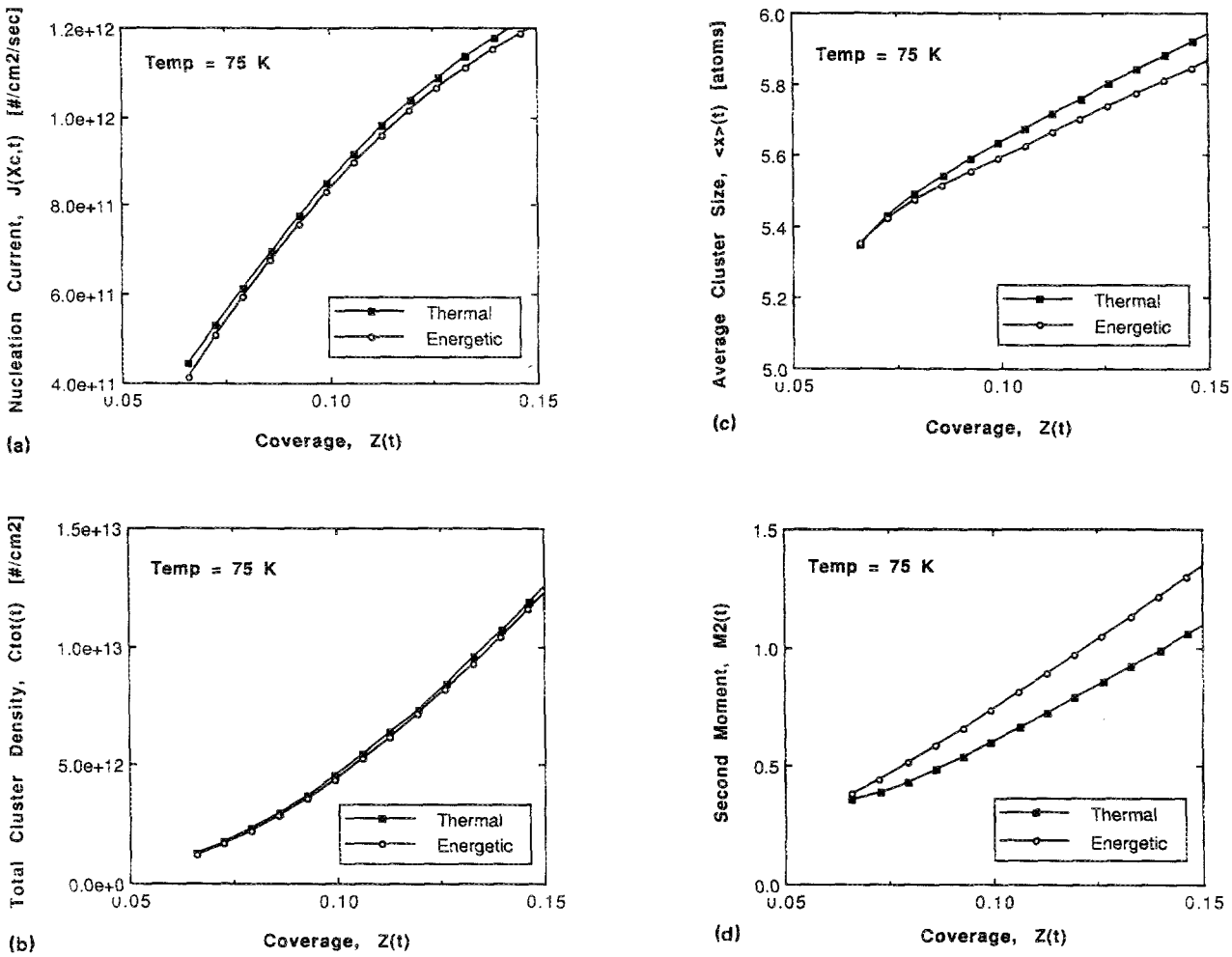

FIG. 4. (a) The influence of cluster dissociation on the nucleation rate $J(X_c,t)$. The thermal case corresponds to $\lambda(E) = 0$, while the energetic case has $\lambda(E) = 1.5\times 10e^{-8}$ cm. (b) The influence of cluster dissociation on the total cluster density $C_{\text{tot}}(t)$. The thermal case corresponds to $\lambda(E) = 0$, while the energetic case has $\lambda(E) = 1.5\times 10e^{-8}$ cm. (c) The influence of cluster dissociation on the average cluster size $\langle x\rangle(t)$. The thermal case corresponds to $\lambda(E) = 0$, while the energetic case has $\lambda(E) = 1.5\times 10e^{-8}$ cm. (d) The influence of cluster dissociation on the second moment (i.e., variance) of the cluster size distribution $M_2(t)$. The thermal case corresponds to $\lambda(E) = 0$, while the energetic case has $\lambda(E) = 1.5\times 10e^{-8}$ cm.

One should realize that the selected values chosen for the dissociation and trapping parameters, $\lambda(E)$ and $p(E)$, remain open to scrutiny. Molecular dynamics simulations for low-energy ion irradiation studies could possibly be designed to provide actual estimates of $\lambda(E)$ and $p(E)$ as functions of bombardment energy E. Recent computer simulations indicate that $\lambda(E) \simeq 3\text{–}5\times 10^{-8}$ cm for 100 eV Cu neutrals incident on a (100) Cu surface.[23] Our choice of $\lambda(E) = 1.5\times 10^{-8}$ cm enables us to model dissociation in the Au/NaCl system with Eq. (28), greatly simplifying one aspect of our computations.[21] Again, by choosing a range of $\lambda(E)$ and $p(E)$ values, we are able to study the effects of cluster dissociation and surface defect production, not the details.

The activation energies E_d^T and E_T must also be accurately determined for more quantitative studies. Assuming that E_d^T is equivalent to an activation energy for surface-vacancy diffusion is probably not a bad approximation. Nonetheless, the manner in which traps or other defects influence the nucleation kinetics may be more complicated than currently modeled. Modulated-beam mass spectrometry and thermally stimulated desorption measurements have been used to determine the binding energy of preferred adsorption sites produced by ion irradiation,[26,27] thus promising better estimates of E_T.

V. CONCLUSIONS

Since a variety of synergistic effects manifest themselves during an energetic particle deposition process, it is not surprising that some discrepancies exist in the experimental literature. The computational model described in this paper attempts to identify the separate influences of surface defect production and cluster dissociation reactions. Surface defect production increases the nucleation rate, leading to larger nuclei densities, smaller average sizes, and a narrower size

distribution. At low substrate temperatures of 75 K, where thermally activated processes are not dominant, cluster dissociation is found to decrease the nucleation rate, promoting smaller island densities. The destructive nature of the dissociation process, however, leads to smaller average sizes and a more disperse size distribution. At higher temperatures, dissociation is found not to influence the nucleation kinetics.

Although energetic particle bombardment may enhance adatom diffusivities, our dissociation results imply that such a phenomena might become a secondary effect at higher substrate temperatures. The influence of low-energy particle–surface interactions on the later stages of thin film formation could also be significantly different from the early stages, since cluster growth and mobility coalescence reactions must be considered. Energetic particle deposition is remarkably different from thermal particle deposition as exemplified by the differences in calculated cluster size distributions and nucleation kinetics.

[1] D. M. Mattox, in *Plasma–Surface Interactions and Processing of Materials*, edited by O. Auciello, A. Gras-Marti, J. A. Valles-Abarca, and D. L. Flamm (Academic, The Netherlands, 1990), p. 377.
[2] J. E. Greene, S. A. Barnett, J.-E. Sundgren, and A. Rockett, in *Plasma–Surface Interactions and Processing of Materials*, edited by O. Auciello, A. Gras-Marti, J. A. Valles-Abarca, and D. L. Flamm (Academic, The Netherlands, 1990), p. 281.
[3] J. E. Greene and S. A. Barnett, J. Vac. Sci. Technol. **21**, 285 (1982).
[4] J. E. Greene, CRC Crit. Rev. Solid State Mater. Sci. **11**, 189 (1983).
[5] J. E. Greene, T. Motooka, J.-E. Sundgren, D. Lubben, S. Gorbatkin, and S. A. Barnett, Nucl. Instrum. Methods Phys. Res. B **27**, 226 (1987).
[6] E. Krikorian and R. J. Sneed, Astrophys. Space Sci. **65**, 129 (1979).
[7] M.-A. Hasan, S. A. Barnett, J.-E. Sundgren, and J. E. Greene, J. Vac. Sci. Technol. A **5**, 1883 (1987).
[8] T. C. Huang, G. Lim, F. Parmigiani, and E. Kay, J. Vac. Sci. Technol. A **3**, 2161 (1985).
[9] V. N. E. Robinson and J. L. Robins, Thin Solid Films **20**, 155 (1974).
[10] A. J. Donohoe and J. L. Robins, J. Cryst. Growth **17**, 70 (1972).
[11] B. F. Usher and J. L. Robins, Thin Solid Films **155**, 267 (1987).
[12] H. Schmeisser, Thin Solid Films **22**, 83 (1974).
[13] H. Schmeisser, Thin Solid Films **22**, 99 (1974).
[14] B. F. Usher and J. L. Robins, Thin Solid Films **149**, 351 (1987).
[15] B. F. Usher and J. L. Robins, Thin Solid Films **149**, 363 (1987).
[16] B. Lewis and M. R. Jordan, Thin Solid Films **6**, 1 (1970).
[17] B. N. Chapman and D. S. Campbell, J. Phys. C **2**, 200 (1969).
[18] G. E. Lane and J. C. Anderson, Thin Solid Films **26**, 5 (1975).
[19] G. E. Lane and J. C. Anderson, Thin Solid Films **57**, 277 (1979).
[20] M. Harsdorff and W. Jark, Thin Solid Films **128**, 79 (1985).
[21] C. A. Stone, Ph. D. Dissertation, University of California, Los Angeles, 1990.
[22] C. A. Stone and N. M. Ghoniem, Metall. Trans. A **20A**, 2609 (1989).
[23] P. S. Chou (in preparation).
[24] R. Niedermayer, Angew. Chem. Int. Ed. Engl. **14**, 212 (1975).
[25] M. Marinov, Thin Solid Films **46**, 267 (1977).
[26] S. A. Barnett, H. F. Winters, and J. E. Greene, Surf. Sci. **165**, 303 (1986).
[27] S. A. Barnett, H. F. Winters, and J. E. Greene, Surf. Sci. **181**, 596 (1987).